LNO_x in deep convection as simulated by an explicit charging and discharge lightning scheme implemented within the WRF-ARW model

Fengxia Guo[1,*], Edward Mansell[2], Alexandre Fierro[2]

1. Collaborative Innovation Center on Forecast and Evaluation of Meteorological Disasters, Nanjing University of Information Science & Technology, Nanjing, China
2. NOAA/National Severe Storms Laboratory, Norman, Oklahoma, U.S.A.

ABSTRACT: In order to study the characteristics of LNO_X in deep convection, this study presents numerical simulations of the generation and transport of LNO_X via a new explicit lightning model implemented within WRF-ARW featuring explicit inductive and non-inductive charging processes. The test case is the 10 July 1996 STERAO storm. The isolated storm evolved from a multicellular thunderstorm to a quasi-supercell. Three convective cells were initiated in the domain, oriented northwest-southeast. After one hour, the updraft of middle cell was weak, with correspondingly low liquid water content and low ice crystal and graupel mixing ratios, resulting in less lightning and NO_X. The other two stronger cells had more lightning and LNO_X production. In general, LNO_X was distributed in the net charge regions, but did not follow an obvious relationship with charge density. The peak LNO_X concentration (2.0-5.0 ppbv) was near the top of the updraft within a region of relatively high ice crystal and graupel concentration. Another peak in LNO_X (1.0-2.5ppbv) was located in a region extending from the ground up to an altitude of 3 km, under the lower positive charge center. The stronger the cell is, the more obvious the lower peak LNO_X becomes. LNO_X was lower (0.25-0.5ppbv) between 3-7km height, corresponding to the strong updraft region and reduced production. The LNO_X distribution within this simulated storm exhibits a noticeable "C" shape. After 2-4 h of simulation, the storm gradually evolved from a multicellular thunderstorm to a quasi-supercell. The maximum LNO_X content exceeded 5ppbv for a period within a broader area.

INTRODUCTION

Lightning-produced NO_X (LNO_X) is a major source of tropospheric nitrogen oxides (NO_X=NO+ NO_2). Research for LNO_X is helpful to understand the feedback of lightning activity to climate。

Zel'dovich and Raizer [1967] first provided the chemical equations of LNO_X. Nitric oxide (NO) is produced in very hot (about 30,000K) lightning channels due to oxygen (O_2) and nitrogen (N_2) dissociation. As the channels cool to 3000-4000 K, NO is formed in the resulting plasma and is "frozen in" during the subsequent cooling to ambient temperature. Within seconds NO is converted to NO_2 by

* Contact information: Fengxia Guo, Collaborative Innovation Center on Forecast and Evaluation of Meteorological Disasters, Nanjing University of Information Science & Technology, Nanjing, China, Email: guofxnj@gmail.com

reaction with ambient ozone (O_3). NO_2 can be photolysed back to NO during daytime. An equilibrium is reached after about 100 s, known as the photostationary state. Wang et al. [1998] studied the production of NO by means of arc discharges in the laboratory. Their results were accepted to be the most accurate results among similar experiments. They found that production of NO_2 was less than 10% of the production of NO in arc discharge. So, most research has studied the characteristics of LNO_X through estimating the production of lightning-produced NO.

Many previous studies implement LNO_X scheme in high resolution cloud-resolving models. The first type of parameterization distributes LNO_X based on observed or simply-paramerized lightning flash rate. [Pickering et al. 1998, Wang and Prinn 2000, DeCaria et al., 2000,2005]. The second type of LNO_X parameterization in cloud model is based on explicit microphysical charge separation and discharge mechanisms. Zhang et al. [2003] first added a LNO_X parameterization into 3-D Storm Electrification Model (SEM) with an explicit and completed charging mechanism parameterization. An unbranched lightning channel propagated along the electrical field vector and presented quasi-vertically according to Kasemir [1960, 1983]. The lightning discharge parameterization only simulated IC flashes, and without branching could not include horizontal channels, which can extend to tens of kilometers. LNO_X distributed in a given volume around lightning channel in proportion to lightning released energy and neutralized charge according to a certain ratio. NO production was set to be 9.2×10^{16} molecules/J. For their simulation, a number of chemical reactions among NO, NO_2 and O_3 were considered. Simulated lightning frequency was much less than that observed.

Barthe et al.[2007] implemented an explicit LNO_X scheme in the 3-D mesoscale model Meso-NH [Barthe et al.,2005] with a complete electrification and lightning flash scheme [Barthe et al. 2005]. The electric charges were carried by each of the five hydrometeor categories of the mixed phase microphysical scheme. They were mostly separated by elastic ice-graupel collisions, known as a non-inductive process. The lightning flash scheme, based on MacGorman et al. [2001] consisted of two parts: a quasi-vertical bidirectional leader and growing branching streamers. The leader was triggered and propagates according to the ambient electrical field. Branches were generated by an iterative algorithm. The maximum number of branches at a given distance from the initiation point obeyed a fractal law. The scheme mimics branches and especially the horizontal extension of IC flashes. This model adapted the method of Wang et al [1998], where the LNO_X production was proportional to the lightning flash length and depended on the atmospheric pressure. No chemistry was considered in their model.

Barth et al. [2007] simulated the storm case of 10 July 1996 STERAO (Stratopheric-Tropospheric Experiment: Radiation, Aerosols, and Ozone) by using eight different cloud models and described the intercomparison to examine transport of six species of chemical substances. All but one of these models considered the reactions of chemical substances, and six of them included some type of lightning-produced NO_X. The WRF-AqChem and UMd/GCE followed DeCaria et al. [2005]. C. Wang's convective cloud model with chemistry followed the disk model of Wang and Prinn [2000]. M. Leriche and S. Cautenet used the scheme of Pickering et al.[1998] in RAMS with an assumed NO production rate of 1113 and 111 moles NO per each CG and IC flash, respectively. J.-P.Pinty, C.Barthe and C.Mari added NO in Meso-NH along the lightning flash path as a function of the pressure and the channel length as suggested by Wang et al [1998]. The average production of NO was 36moles per flash for both CG and IC flashes.

In 3-D SEM (Storm Electrification Model) [Helsdon and Farley, 1987, and Helsdon et al., 2001] energy dissipation can be determined by calculating the electrical energy just before and immediately after the discharge. Lightning-produced NO production (9×10^{16}NO molecules J^{-1} at sea level) is proportional to this electrical energy and pressure, and is limited to the immediate vicinity of the lightning channel. For this simulation, the NO production ranged from 5 to 351 moles NO per flash with a mean of 97 moles.

The results of Barth et al. [2007] indicated that models that included lightning production of NO_X reasonably predict NO_X mixing ratios in the anvil compared with observations.

In order to study the characteristic of LNO_X in deep convection, this paper presents numerical simulations of the generation and transport of LNO_X via a new explicit lightning model implemented within WRF-ARW featuring explicit inductive and non-inductive charging processes [Fierro et al. 2013]. The discrete lightning discharge scheme of MacGorman [2001] was also incorporated into the model. The lightning-generated NO_X followed the scheme of Wang et al. [1998] with assumptions of channel length within each grid cell. The test case of the 10 July 1996 STERAO storm was simulated.

DESCRIPTION OF THE MODEL

Lightning parameterization

Fierro et al. [2013] implemented an explicit lightning physics within the Weather Research and Forecast (WRF) model. Charging of hydrometeors consists of five distinct non-inductive parameterizations, polarization of cloud water and the exchange of charge during collisional mass transfer (Mansell et al. 2010, Saunders and Peck 1998, Brooks et al. 1997). No screening layer parameterization was used for these simulations. The discharge process employs concepts adapted from two well-documented bulk lightning models [MacGorman,1994, MacGorman et al.,2001], whereby charge reduction is imposed within a prescribed volume centered at grid points characterized by electric field magnitudes exceeding a given breakdown threshold.

In order to simulate LNO_X, we employ lightning parameterization adapted from MacGorman [2001] in Ferro et al. [2013] model. Since the scheme produces few CG flashes, IC flashes were hybridized to allow a net discharge. Normally IC flashes would be limited to have equal and opposite charge deposition at the positive and negative ends. If the immediate region of the flash carried a net charge, however, the IC flash was allowed to act against that net charge if possible. For example, if the storm region had net positive charge, and the flash had more positive than negative charge available for discharge, then the flash could deposit excess negative charge into the positive region. Otherwise, IC flashes were restricted to be overall neutral.

The lightning parameterization adapted from MacGorman [2001] just can mimic the gross structure of flashes, not the detailed development of lightning channels. In this scheme, instead of stopping at larger ambient electric field magnitudes, extensive flash development can continue in regions having a weak ambient electric field but a substantial charge density and consistent electric potential, so the extension of lightning channel simulated by the new parameterization is same as lightning structure observations. Although the choice of parameter values affects the simulated lightning structure, the qualitative features of simulated flash structure are similar to those of observed lightning as long as the parameter values are consistent with the larger electric field magnitudes measured in storms and with simulated charge densities produced over reasonably large regions. The new parameterization is computationally efficient, but less so than the bulk lightning model [Fierro et al.] because each flash is computed sequentially with a recalculation of the electric potential after each flash.

LNO_x parameterization

We employ the LNO_X parameterization adapted from Wang et al. [1998]. NO_X is produced as a function of lightning channel length and pressure with a scaling based on the amount of charge deposited in a given grid cell. The molecule number $n_{NO}{}''$ (unit: 10^{21} molecules/m) produced by per meter of lightning channel is,

$$n_{NO}{}''\left(i,j,k\right) = a + bP\left(i,j,k\right) \tag{1}$$

Where P is pressure (unit: Pa), a=0.34, b=1.30, and i,j,k represent coordinates of discharge grid in x,y and z, respectively. The lightning-NO (unit: mol) of each grid volume is,

$$n_{NO}{}'\left(i,j,k\right) = l_{chan} \times n_{NO}{}''\left(i,j,k\right) / N_A \tag{2}$$

where l_{chan} is channel length (m) and is taken as the horizontal grid spacing dx, N_A is Avogadro constant, equal to 6.022×10^{23}mol^{-1}.

The volume concentration of lightning-generated NO of each grid volume is,

$$n_{NO}\left(i,j,k\right) = \delta\rho'\left(i,j,k\right) \times n_{NO}{}'\left(i,j,k\right) \times M_{air} / \left(\rho_{air} \times \Delta V\right) \tag{3}$$

where $M_{air} = 28.96 \times 10^{-3}\, kg\ mol^{-1}$, is mole mass of air. ΔV is grid volume (m^3), equal to $dx \times dy \times dz$, dx, dy and dz (unit: m) are grid distance in x, y and z direction, respectively. ρ_{air} is air density (kg m^{-3}).

$$\delta\rho'\left(i,j,k\right) = \left(\left|\Delta\rho_{\pm}\left(i,j,k\right)\right|\right) / \delta q_0 \tag{4}$$

It is a ratio of neutralized charge at each discharge grid to δq_0. $\Delta\rho_+\left(i,j,k\right)$ is the deposited charge density at a grid point at the positive end of the lightning, and $\Delta\rho_-\left(i,j,k\right)$ is the deposited charge density at a grid point at the negative end. δq_0 is a referenced charge density to scale the NO production. In this paper, $\delta q_0 = 0.5nCm^{-3}$. The introduction of δq_0 is based on the laboratory result of Wang et al. [1998]. Their study showed that NO production is 15×10^{16}mol J^{-1} when current in lightning channel is 10kA, while, NO production is 40×10^{16} mol J^{-1} when current in lightning channel is 30kA. So, it can be inferred that a linear relationship may exist between NO production and lightning energy (current). In this paper, the neutralized charge is used to represent lightning energy, and together with a standard referenced charge density δq_0 to correct NO production at each grid. This method is reasonable and can avoid the virtual high of simulation NO production.

SIMULATION OF THUNDERSTORM CASE IN STERAO

The storm case of 10 July 1996 STERAO (Stratospheric-Tropospheric Experiment: Radiation, Aerosols, and Ozone) is simulated by using the WRF-ARW including explicit charging and discharge parameterization within the NSSL 2-moment microphysics scheme (Mansell et al. 2010). A major purpose of STERAO was to study the effect of lightning on chemical constituents in middle and upper troposphere, especially LNO_X and NO_X transport from boundary layer. Observations of the storm were obtained from several platforms including the CSU CHILL radar, the ONERA lightning interferometers, the NOAA WP3D aircraft and UND Citation aircraft [Dye et al., 2000]. This thunderstorm was observed near the Wyoming-Nebraska-Colorado border. The isolated storm evolved from a multicelluar thunderstorm to a quasi-supercell.

Previous model simulations have proven to successfully represent the observed storm [Skamarock et al. 2000, 2003, Barth et al. 2001, 2007]. The environmental was assumed to be homogeneous, thus a single profile observed by aircraft and radiosonde was used for initialization [Skamarock et al., 2000]. The convection is initiated with 3 warm bubbles (3℃ perturbation) oriented in a NW to SE line following Skamarock et al.[2000].

Hydrometeors

Figure 1 shows vertical cross sections of hydrometeor mixing ratios at 1 hour and 3.5 hours. During the multicellular stage (Figure 1a), three aligned convective cells are in NW-SE direction. Each cell top reaches about 13 km altitude and has a horizontal extent of 20 km. The central cell contains a low cloud droplet mixing ratio compared to that of the two other cells, so its convection is weak.

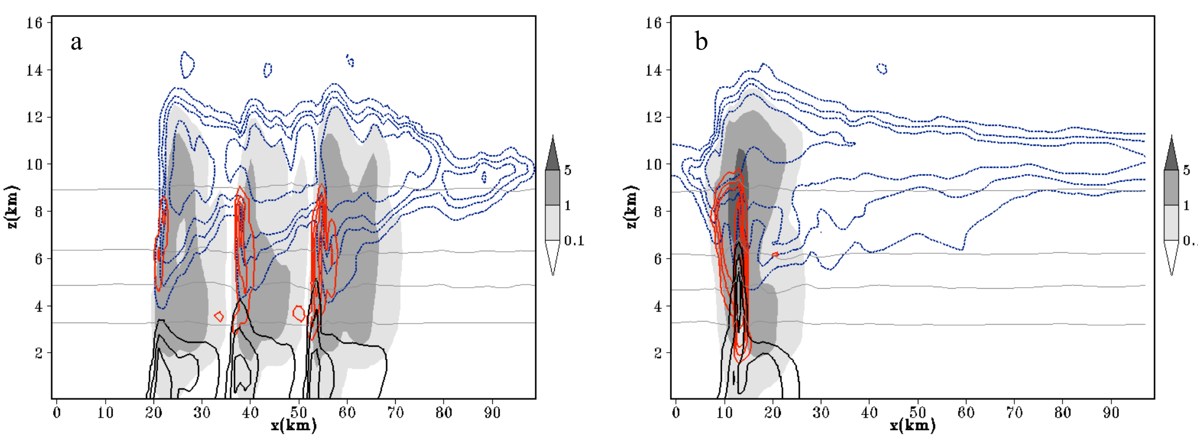

Figure 1. Partial vertical along-wind cross section at (a) 1 hour and (b) 3.5 hours of hydrometeor mixing ratios. Colored areas, blue dashed lines, red solid lines and black solid lines represent graupel, pristine ice and snow, cloud droplet and rain drop mixing ratios respectively. The mixing ratio contours are 0.1, 0.5, 1 and 2 g kg^{-1} for pristine ice and snow, cloud droplets and rain drops. Grey solid lines represent 0℃, -10℃, -20℃ and -40℃ from upper to lower.

All of them have the anvil comprised of ice crystal and snow. The anvils of the northwestern and central cells overlap the cloud top of the adjacent downwind cell, and anvil of southeast cell stretches downwind to 30 km. For the middle cell, the cloud droplet mixing ratio was relatively low, and without obvious rain. At the same time, mixing ratios of graupel and hail are relatively low, less than 5 g kg^{-1} in center, due to the lower amounts of cloud water. So, charging process is weak, and less LNO is generated. While the two other cells with little rain (0.1 g kg^{-1}) and higher cloud water, and supercooled water up to the -40℃ layer. So, graupel and hail between -30℃ and -40℃ grow by riming, and their mixing ratios exceed 5 g kg^{-1}. The anvil of the sourtheast cell has greater ice crystals and snow contents than two other cells and stretches farther downwind. The storm develops supercell characteristic at about 2.5 h of simulation (not shown), and the anvil stretches downwind for about 70 km. In the core convection area, mixing ratios of ice crystal and snow reach about 2 g kg^{-1} near 10 km, cloud droplet top reaches near -40℃ layer with mixing ratio exceeding 0.5 g kg^{-1}, and graupel and hail between 4 and 10 km have mixing ratio reaching 1-5 g kg^{-1}. Rain distributes in the area near the surface, and its mixing ratio reach to 0.1 g kg^{-1}. During the supercellular stage (Figure 1b), the anvil extend on 100 km in the NW-SE direction. At 10.0 km altitude, the pristine ice and snow mixing ratio reaches 2 g kg^{-1}. The maximum graupel mixing ratio remains around 5 g kg^{-1} at 6-10 km. The cloud droplet and the rain drop mixing ratios reach 2 g kg^{-1} and 1.5 g kg^{-1} respectively. All the results are consistent with the simulation made by Barthe et al. [2007] using Meso-NH.

Charge structure and reflectivity

Figure 2 shows a vertical cross section of total charge density and of reflectivity through the three multicell cores, after 1 hour and 3.5 hours of simulation. During the multicellular stage (Figure 2a), each cell is characterized by complex structure dominated by a normal dipole but with a weaker upper negative charge layer. This structure is similar as the highly stratified structure discussed by Stolzenburg et al. [1998] and different from the inverted dipole structures simulated by Barthe et al. [2007]. Barthe et al. [2007] adopted the non-inductive charging results of Takahashi [1978] and neglected the inductive mechanism. All of these in addition to different models and microphysics can cause distinctly different results. The electrification in the southeastern cell is strongest. The magnitudes of its positive and negative charge density reach 1.0 nC m^{-3}. During the multicellular stage (Figure 2b), the charge structure is an inverted dipolar. During the two stages, the main positive and negative charge regions of cells are all located in the upper of the strongest reflectivity region, and the charge regions are limited in the area that reflectivity is more than 40 dBZ.

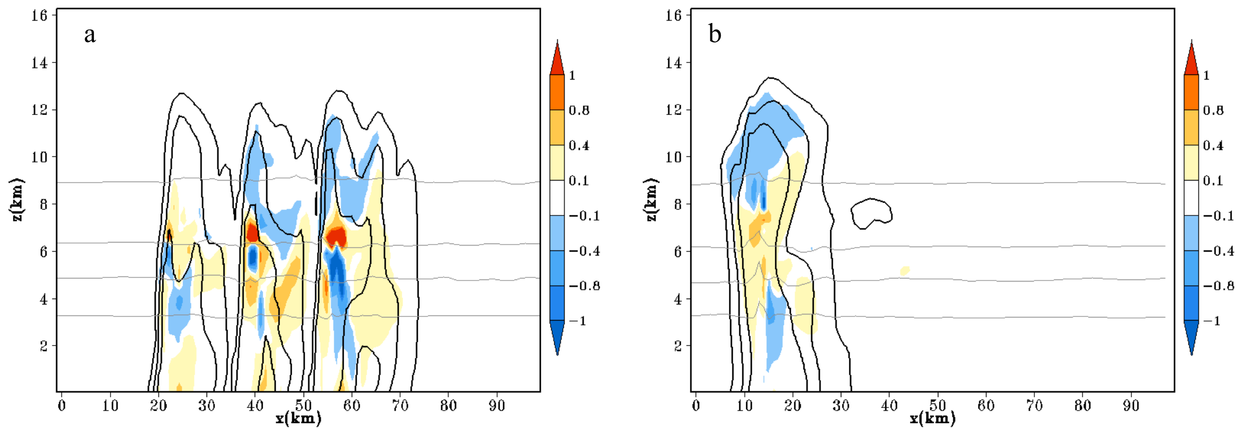

Figure 2 . Partial vertical along-wind cross section at (a) 1 hour and (b) 3.5 hours of net charge density (colored areas, unit: nC m^{-3}) and radar reflectivity (contours: 20 dBZ, 40 dBZ and 60 dBZ). Grey solid lines represent 0℃, -10℃, -20℃ and -40℃ from upper to lower.

LNO_x production

During the multicellular stage, in the strongest convection regions (Figure 3a), LNO_X distribution is limited in the whole charge region compared with Figure 2a. In the stronger convection regions (Figure 3b), LNO_X mainly distributes in the upper of cloud. The peak values of NO_X of both cross sections reached 2.0-5.0ppbv. The environmental of NO_X is about 0.4-0.6ppbv from ground to 2 km height [Barthe et al., 2007]. The LNO_X distribution within this simulated storm results from production by lightning and subsequent transport by both updrafts and downdrafts. Although environmental NOx is not included, an enhancement by lightning would certainly be evident in the anvil exhaust region as well as in downdrafts reaching the surface. [Huntrieser et al. 2002],.

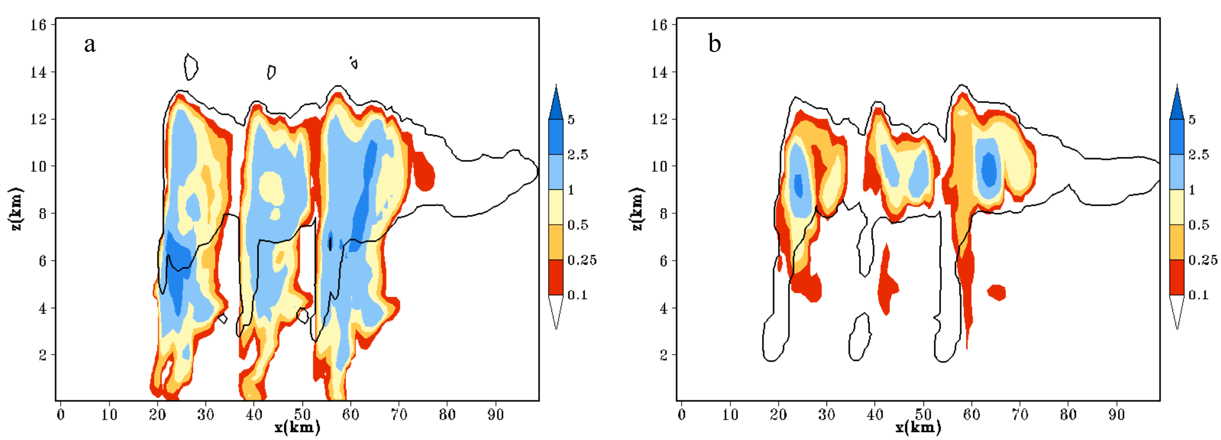

Figure 3. Along-wind vertical cross section of the NO_x in the multicellular stage (colored areas in pptv). The cloud limit is outlined (thick solid line). (a. the strongest convection region; b. the stronger updraft region)

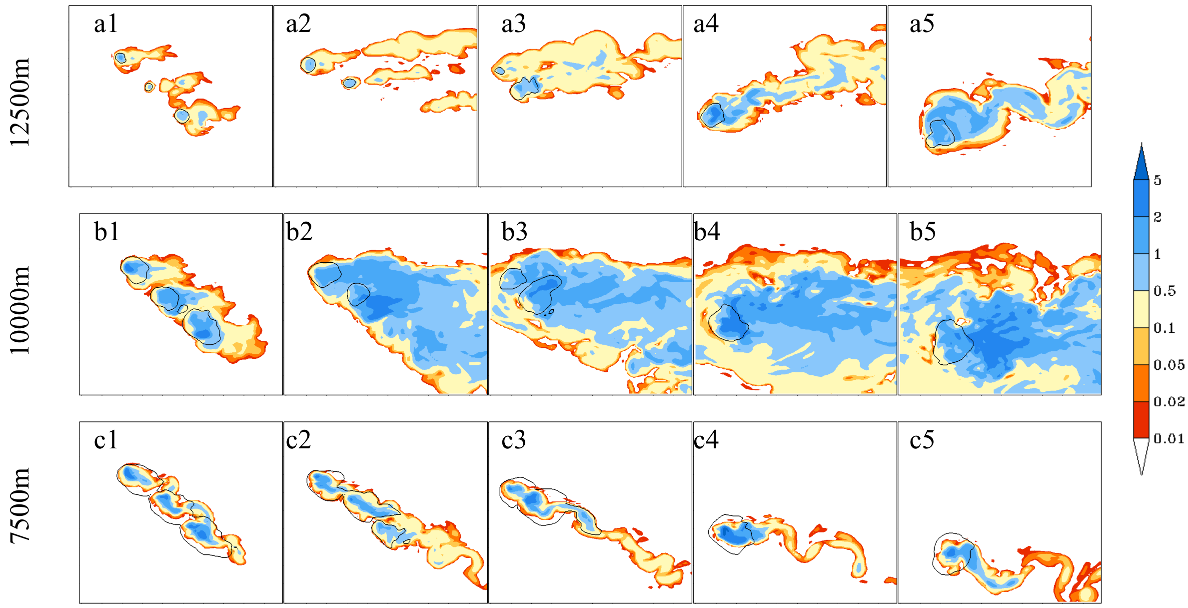

Figure 4. Horizontal cross sections at (top) 12,500 m (a), (middle) 10,000 m (b) and (bottom) 7500 m (c) of the hourly LNO_x concertration in logarithmic scale at 1,2,3,4 and 5 hours. Solid black lines are areas with reflectivity larger than 20 dBZ. Every horizontal domain is 100 km×100 km.

The hourly LNO_X field is displayed through a series of plots in Figure 4 for three elevations: 12.500 m, 10,000 m and 7,500 m. After one hour of simulation, NO_X is produced in each cell and their peak values are almost limited the convection centers. The NO_X at 10 km height is the largest (1~2ppbv). Just a little LNO_X is transported to downwind. After 2-4 h of simulation, the storm gradually evolved from a multicellular thunderstorm to a quasi-supercell. More and more LNO_X is produced with the storm, and the peak value of LNO_X exceed 5 ppbv for a short period. Due to the atmospheric turbulence and advection, the LNO_X is gradually transported and diluted. So, the region of LNO_X extends to downwind in the anvil in a large area, and the peak of LNO_X is not more than 5 ppbv at the later time.

CONCLUSIONS

This study presents a numerical simulation of the generation and transport of LNO_X via a new explicit lightning model implemented within WRF-ARW featuring explicit inductive and non-inductive charging processes. Via simulation of the 10 July 1996 STERAO storm, it is indicated that LNO_X is mainly produced in the charge region and then diluted and transported to downwind in the anvil in a large area.

ACKNOWLEDGMENTS

This work is supported by The National Natural Science Foundation of China (No.41275008), National Key Basic Research Program of China (No.2014CB441403), the R&D Special Fund for Public Welfare Industry (GYHY201306069) and Basic Scientific Research Operating Expense of CAMS (No.2010Z004).

REFERENCES

Barth, M. C., Kim, S.-W., Wang. C., et al., 2007: Cloud-scale model intercomparison of chemical constituent transport in deep convection. *Atmos. Chem. Phys.*, 7, 4709–4731.

Barthe, C., Molinie, G., and Pinty, J.-P., 2005: Description and first results of an explicit electrical scheme in a 3D cloud resolving model. *Atmos. Res.*, 76, 95–113.

Barthe, C., Pinty, J.-P., and Mari, C., 2007: Lightning-produced NOx in an explicit electrical scheme tested in a Stratosphere-Troposphere Experiment: Radiation, Aerosols, and Ozone case study. *J. Geophys. Res.*, 112, D04302, doi:10.1029/2006JD007402.

Brooks, I. M., C. P. R. Saunders, R. P. Mitzeva, and S. L. Peck, 1997: The effect on thunderstorm charging of the rate of rime accretion by graupel. *Atmos. Res.*, **43**, 277–295.

DeCaria, A. J., Pickering, K. E., Stenchikov, G. L., Scala, J. R., Stith, J. L., Dye, J. E., Ridley, B. A., and Laroche, P., 2000: A cloud-scale model study of lightning-generated NOx in an individual thunderstorm during STERAO-A. *J. Geophys. Res.*, 105,11 601–11 616.

DeCaria, A. J., Pickering, K. E., Stenchikov, G. L., and Ott, L. E., 2005: Lightning-generated NOx and its impact on tropospheric ozone production: A 3-D modeling study of a STERAO-A thunderstorm. *J. Geophys. Res.*, 110, D14303, doi:10.1029/2004JD005556.

Fierro, Alexandre O., Edward R. Mansell, Donald R. MacGorman, Conrad L. Ziegler, 2013: The implementation of an explicit charging and discharge lightning scheme within the WRF-ARW model: Benchmark simulations of a continental squall Line, a tropical cyclone, and a winter storm. *Mon. Wea. Rev.*, 141, 2390–2415.

Helsdon Jr., J. H. and Farley, R. D., 1987: A numerical modeling study of a Montana thunderstorm, 2, Model results vs. observations involving electrical aspects. *J. Geophys. Res.*, 92, 5661–5675.

Helsdon Jr., J. H.,Wojcik,W. A., and Farley, R. D., 2001: An examination of thunderstorm charging mechanisms using a two-dimensional storm electrification model. *J. Geophys. Res*., 106, 1165–1192.

Huntrieser, H., et al., 2002: Airborne measurements of NOx, tracer species, and small particles during the European Lightning Nitrogen Oxides Experiment. *J. Geophys. Res.*, 107(D11), 4113, doi:10.1029/2000JD000209.

Kasemir, H. W., 1960: A contribution to the electrostatic theory of a lightning discharge. *J. Geophys. Res.,* 65, 1873–1878.

Kasemir, H. W., 1984: Theoretical and experimental determination of field,charge and current on an aircraft hit by natural and triggered lightning. Preprints, *Int. Aerospace and Ground Conf. on Lightning and Static Electricity,* Orlando, FL, National Interagency Coordinating Group, 2.1–2.10.

MacGorman, D. R., and D. W. Burgess, 1994: Positive cloud-to-ground lightning in tornadic storms and hailstorms. *Mon. Wea. Rev.,* 122, 1671–1697.

MacGorman, Donald R., Jerry M. Straka, Conrad L. Ziegler, 2001: A lightning parameterization for numerical cloud models. *J. Appl. Meteor.*, 40, 459–478.

Mansell, E. R., C. L. Ziegler, and E. C. Bruning, 2010: Simulated electrification of a small thunderstorm with two-moment bulk microphysics. *J. Atmos. Sci.,* **67**, 171–194.

Pickering, K. E., Wang, Y., Tao, W.-K., Price, C., and M¨uller, J.-F., 1998: Vertical distributions of lightning NOx for use in regional and global chemical transport models. *J. Geophys. Res*., 103, 31 203–31 212.

Saunders, C. P. R., and S. L. Peck, 1998: Laboratory studies of the influence of the rime accretion rate on charge transfer during crystal/graupel collisions. *J. Geophys. Res*., **103**, 13 949–13 956.

Stolzenburg, M., W. D. Rust, and T. C. Marshall, 1998: Electrical structure in thunderstorm convective regions: 1. Mesoscale convective systems. *J. Geophys. Res.*, 103, 14,059– 14,078.

Wang Y, DeSilva W, Goldenbaum G C, et al., 1998: Nitric oxide production by simulated lightning: dependence on current, energy, and pressure. *Journal of Geophysical Research*, 103(19): 149-159.

Wang, C. and Prinn, R., 2000: On the roles of deep convective clouds in tropospheric chemistry. *J. Geophys. Res.*, 105(D17), 22 269–22 298.

Zel'dovich Y B, Raizer Y P., 1967: Physics of shock waves and high temperature hydrodynamic phenomena. *San Diego: Academic*, 566-571.

Zhang, X., Helsdon Jr., J. H., and Farley, R. D., 2003: Numerical modeling of lightning-produced NOx using an explicit lightning scheme: 2. Three-dimensional simulation and expanded chemistry. *J. Geophys. Res.*, 108(D18), 4580, doi:10.1029/2002JD003225.